ARTICLE

OBC
www.rsc.org/obc

Relative DNA binding affinity of helix 3 homeodomain analogues, major groove binders, can be rapidly screened by displacement of prebound ethidium bromide. A comparative study

Yong-Ho Shim,[a] Paola B. Arimondo,[b] Alain Laigle,[c] Anna Garbesi[d] and Solange Lavielle*[a]

[a] *UMR 7613 CNRS – Paris VI, Case 182, Université P. et M. Curie, 4, Place Jussieu, 75005 Paris, France. E-mail: lavielle@ccr.jussieu.fr; Fax: 33 1 44 27 71 50; Tel: 33 1 44 27 55 35*

[b] *UMR 5153 CNRS, MNHN USM0503, INSERM U565, 43 rue Cuvier, 75005 Paris, France*

[c] *UMR 7033 CNRS – Paris VI, Case 138, Université P. et M. Curie, 4, Place Jussieu, 75005 Paris, France*

[d] *ISOF, Area della Ricerca CNR, Via P. Gobetti, 101, 40129 Bologna, Italy*

Received 17th November 2003, Accepted 7th January 2004
First published as an Advance Article on the web 12th February 2004

The binding affinity for a 12-bp dsDNA of *Antennapedia* helix 3 analogues, major groove binders, has been measured by displacement of prebound ethidium bromide, a fluorescent displacement assay proposed for minor groove binders by Boger *et al.* (*J. Am. Chem. Soc.*, 2000, **122**, 6382–6394). Relative binding affinities determined by this method were compared to those obtained by gel mobility shift and footprinting assays for the 12-bp dsDNA and a 178-bp DNA fragment. The present work demonstrates that the fluorescence displacement assay is suitable for rapid screening of major groove binders, even though about 60 to 70% of the prebound ethidium bromide is displaced by these peptides. Total (100%) displacement of ethidium bromide was serendipitously achieved by addition in the peptide sequence, at the N-terminus, of a *S*-3-nitro-2-pyridinesulfenyl-*N*-acetyl-cysteine residue. *S*-3-nitro-2-pyridinesulfenylcysteine was shown to (i) bind to dsDNA with a micromolar affinity and (ii) direct within DNA grooves a peptide with no affinity for dsDNA.

Introduction

Sequence specific DNA ligands that antagonize DNA/protein interactions represent potentially powerful means of modulating gene expression. Natural ligands like netropsin and distamycin A (Fig. 1), which bind with remarkable affinity to the DNA minor groove at AT-rich sequences, have been the starting point for the development of small distamycin A analogues, endowed with remarkably increased biological activity and altered sequence specificity,[1] and of a family of hairpin lexitropsines featuring compounds able to bind to eight base pair sites in the minor groove, with very high affinity and to discriminate a one base pair mutation.[2] Specific recognition of DNA sequences has also been achieved by oligonucleotides, which bind in the major groove to homopurine·homopyrimidine sites, forming a triple helix structure.[3] The same type of targets can also be recognized with high affinity and specificity by homopyrimidine peptide nucleic acids (PNAs), which upon helix invasion lead to triplex P-loop complexes.[4] The major groove is also the binding site of many eucaryotic transcription factors whose DNA-binding regions contain one of these structural motifs: zinc fingers, leucine zippers or helix-turn-helix. The last motif is characteristic of homeodomain, a highly conserved DNA binding stretch of about 60 amino acids, which is present in many proteins that regulate gene expression, primarily but not exclusively, during embriogenesis.[5] The homeodomain polypeptides, whose tertiary structure is highly conserved, contain three helices with a turn between helix 2 and 3. Helix 3 makes specific contacts with base pairs in the major groove, while the rather flexible N-terminal arm of the homeodomain contacts two base pairs in the minor groove. The overall structure is locked by hydrophobic residues at the interface among the three helices.[6] Altogether, the specific interactions define a DNA consensus sequence of six consecutive base pairs. Considering *Antennapedia* homeodomain (*Antp* HD), a *Drosophila* transcription factor, the key amino acids of the recognition helix 3 are located at positions 47, 50, 51 and 54 and those of the N-terminal arm at positions 3 and 5. In addition, contacts are made by several amino acids with the backbone phosphates of the DNA binding region.[7,8] The consensus DNA site recognized by the *Antp* HD has the sequence 5′-TAATGG-3′ and the equilibrium binding constant of an *Antp* HD peptide (68 residues) for a duplex oligomer containing the 5′-TAATGG-3′ sequence was found to be $K_d = 1.6 \times 10^{-9}$ M, at 20 °C.[9] Previous

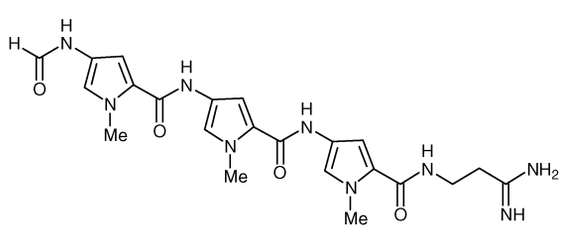

Distamycin A

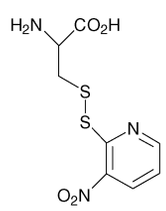

Cys(Npys)

Fig. 1 Chemical structure of distamycin A and 3-nitro-2-pyridinesulfenyl cysteine.

DOI: 10.1039/b314758d

Table 1 Affinity (K_a) of various agents for a 12-bp dsDNA (G1/C2, sequence in Table 2) measured by displacement of prebound ethidium bromide, with in bold the residues of *Antp* helix 3 contacting the base pairs in the cognate DNA site, in italic residues that have been modified

Agent	*n*	$K_a \pm$ SEM [a]/ 10^6 M^{-1}	Sequence	$K_d = 1/K_a$/ 10^{-6} M
1			Arg–Gln–Ile–Lys–**Ile**–Trp–Phe–**Gln**–**Asn**–Arg–Arg–**Met**–Lys–Trp–Lys–Lys	
Distamycin A	2	37 ± 8.5	Confer to Fig. 1	0.027
2	13	16 ± 12	*H_2N–Cys(Npys)*–Arg–Gln–Ile–Lys–**Ile**–Trp–Phe–**Gln**–**Asn**–Arg–Arg–**Met**–Lys–Trp–Lys–Lys–$CONH_2$	0.063
3	1	<0.1	*Ac*–Lys–**Ile**–Trp–Phe–**Gln**–**Asn**–Arg–Arg–**Met**–Lys–$CONH_2$	>10
4	2	<0.1	*Ac–Ala–Ala–Ala*–Lys–**Ile**–Trp–Phe–**Gln**–**Asn**–Arg–Arg–**Met**–Lys–*Ala–Ala–Ala*–$CONH_2$	>10
5	2	<0.1	*Ac–Lys–Lys–Lys*–Lys–**Ile**–Trp–Phe–**Gln**–**Asn**–Arg–Arg–**Met**–Lys–*Lys–Lys–Lys*–$CONH_2$	>10
6	3	2.8 ± 1.1 [b]	*Ac*–Lys–**Ile**–Trp–Phe–**Gln**–**Asn**–Arg–Arg–**Met**–Lys–Trp–**Lys**–Lys–$CONH_2$	0.36
7	3	4.7 ± 3.6 [b]	*Ac*–Arg–Gln–Ile–Lys–**Ile**–Trp–Phe–**Gln**–**Asn**–Arg–Arg–**Met**–Lys–Trp–Lys–Lys–$CONH_2$	0.21
8	2	5.5 ± 4.9 [b]	*Ac–Cys(Acm)*–Arg–Gln–Ile–Lys–**Ile**–Trp–Phe–**Gln**–**Asn**–Arg–Arg–**Met**–Lys–Trp–Lys–Lys–$CONH_2$	0.18
9	2	5.5 ± 2.1	*Ac–Cys(Npys)*–Arg–Gln–Ile–Lys–**Ile**–Trp–Phe–**Gln**–**Asn**–Arg–Arg–**Met**–Lys–Trp–Lys–Lys–$CONH_2$	0.18
Substance P	2	<0.01	H_2N–Arg–Pro–Lys–Pro–Gln–Gln–Phe–Phe–Gly–Leu–Met–$CONH_2$	>100
10	2	1.2 ± 0.4	H_2N–Cys(Npys)–Arg–Pro–Lys–Pro–Gln–Gln–Phe–Phe–Gly–Leu–Met–$CONH_2$	0.83
Cys(Npys)	2	0.3 ± 0.1 [b]	H_2N–Cys(Npys)–OH	3.3

[a] Association constant (K_a) ± standard error of the mean from 2 to 13 (*n*) experiments run in duplicate. [b] Only 60 to 70% of the ethidium bromide is displaced.

43 47 50 51 54 58
Arg-Gln-Ile-Lys-**Ile**-Trp-Phe-**Gln**-**Asn**-Arg-Arg-**Met**-Lys-Trp-Lys-Lys

Peptide **1**

Antp helix 3 homeodomain (residues 43 to 58), with in bold the residues contacting the base pairs in the cognate DNA site

research has shown that the basic 16-amino acid peptide **1**, corresponding to *Antp* helix 3, is efficiently internalized by cells in culture, where it is found mainly in the nucleus and also in the cytoplasm and can be used as a vector for polypeptides, proteins and oligonucleotides.[10]

The aim of the investigation described therein was to measure the affinity of peptide **1** and determine its binding selectivity for oligodeoxynucleotides containing the consensus sequence for the *Antp* HD. It was already known that peptide **1** has a pretty low helicity in water,[11] but it was hypothesized that, in analogy with the behaviour of the basic region of the leucine zipper proteins, helicity might be enhanced in the presence of its specific DNA binding site, consecutive to an induced-fit mechanism.[12] We also envisaged to bias the wild type sequence toward a helical structure by substitution of appropriate residues first with alanine or lysine, whose ability to stabilize this conformation is well documented [13,14] and ultimately by suitably designed amino acids and/or procedures.

The method we choose to estimate the binding affinity of *Antp* helix 3 analogues derived from peptide **1** (Table 1) is based on the decrease of fluorescence, which ensues the displacement from the oligodeoxynucleotide duplex target of prebound intercalator ethidium bromide by a non fluorescent DNA binding compound.[1] Relative binding affinities determined by this technique were then compared to those obtained by gel mobility shift and footprinting assays.

Results and discussion

Ethidium bromide assay

A fluorescent intercalator displacement (FID) assay has been proposed by Boger *et al.*[1] to assess relative or absolute binding affinity of DNA binders. This technique, based on the decrease of fluorescence derived from the displacement of ethidium bromide (BET) from a DNA sequence, has been used to screen ligands specific to DNA minor grooves. Binding affinities obtained by this FID assay have been shown to be in the same range as that obtained with gel retardation assays. Recently, Chaltin *et al.*[15] reported that this FID assay was complementary to the gel retardation assay to select dsDNA binding ligands from a library of unnatural oligopeptides.

Boger *et al.*,[1] using a competitive and a non-competitive binding model, have reported binding constants K_a for distamycin A (Fig. 1), a well-known minor groove ligand, ranging from $K_a = 5$ to 94×10^6 M^{-1}, depending on the DNA sequence, with the trend 5′-ATTAA-3′ < AATAA < AAAAA < AATTT. The *Antp* binding site features the consensus 5′-TAAT core motif, which is also an appropriate binding site for distamycin A. Hence, we used distamycin A as a control molecule, to check if our conditions for fluorescence determination on a droplet (7 μL) of the incubation medium yielded reproducible and accurate values for K_a, when compared to Boger *et al*. reported values.[1] To calculate the K_a value of distamycin A for the 12-base-pair dsDNA sequence (G1/C2, Table 2), containing the *Antp* consensus site, we applied the competitive binding model, with $K_{EB} = 9.6 \times 10^6$ M^{-1},[16,17] and found $K_a = 37 \pm 8.5 \times 10^6$ M^{-1}, a value within those reported for this minor groove ligand toward sites containing the 5′-TAAT core sequence.

Then, in order to investigate the binding properties of *Antp* helix 3 analogues, the affinities of peptide **1** analogues were determined for the 12-base-pair dsDNA (G1/C2) by this FID strategy, using the competitive binding model. Peptide **2** (Table 1) corresponds to the 16-residue *Antp* helix 3 with a Cys(3-nitro-2-pyridinesulfenyl) (Fig. 1) at the N-terminus. Peptide **2** is a functionalised analogue of peptide **1** [10,11] which has been initially proposed by our laboratory for linking, by a disulfide bridge, various substrates to be translocated by *Antp* helix 3 inside a cell. Peptide **2** totally displaced ethidium bromide from the preformed dsDNA–BET complex, its relative affinity K_a was calculated, $K_a = 19 \pm 7 \times 10^6$ M^{-1} (Fig. 2). A dissociation constant (K_d) in the nanomolar range has been previously determined by gel shift analysis for the 68-amino acids *Antp* homeodomain.[9,18] A 100-fold decrease in the affinity

Table 2 DNA targets. Underlined sequences are potential binding sites for *Antp* helix 3 analogues

DNA	Sequence
G1 (12-bp)	5′-GCGTAATG;GCGC-3′
178-bp	5′-CAGCTGGCGAAAGGGGATGTGCTGCAA-GGCGATTAAGTTGGGTAACGCCAGGGTTT-TCCCAGTCACGACGTTGTAAAACGACGGC-CAGTGAGCGCGCGTAATACGACTCACTATA-GGGCGAATTGGGTACCGGGCCCCCCCTC-GAGGTCGACGGTATCGATAAGCTTGATAT-CG-3′

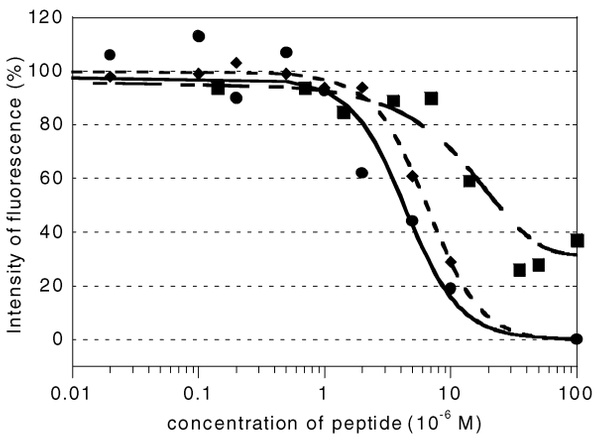

Fig. 2 Ethidium bromide displacement assay by fluorescence spectroscopy (measured at 595 nm with excitation at 514 nm) for a complex of ethidium bromide (4.4×10^{-6} M) with a 12-bp dsDNA (G1/C2, Table 2 at 8.8×10^{-6} M base pairs) in the presence of increasing concentrations of peptide **2** (●, ——), **8** (■, ---) and **9** (◆, ···), concentrations range from 0.1 to 10×10^{-7} M, in a 0.1 M Tris-HCl, 0.1 M NaCl, pH 8 buffer solution, after overnight incubation at 25 °C. The fluorescence is expressed as a percentage of the control fluorescence: for 100% fluorescence (no peptide added) and 0% fluorescence (no DNA). Data reported correspond to typical titration curves for these peptides with each concentration in duplicate and each experiment has been at least run in duplicate.

of the isolated *Antp* helix 3, peptide **2**, was acceptable considering that (i) two residues from the N-terminal sequence of the 68-residues sequence contact the dsDNA in the adjacent minor groove and thus participate to the stabilisation of the dsDNA/homeodomain complex and (ii) the 16-residue sequence (sequence 43 to 59 of *Antp* HD) is mainly in random coil conformation in water. This 16-residue peptide has been reported to be as potent as the 68-amino acid sequence to translocate and address proteins within the nucleus.

A structure–affinity relationship investigation was then performed with a few peptide **2** analogues (Table 1). The shorter peptide **3** corresponding to the core 10-amino acid has no affinity for the dsDNA (G1/C2), concentrations up to 0.1 mM did not at all decrease the ethidium bromide fluorescence. Addition on both the N- and C-terminus sides of three alanines or lysines, two helix inducers or stabilizers, was totally inefficient, both the 16-residue peptides **4** and **5** have no affinity for the G1/C2 dsDNA. The absence of affinity for this dsDNA of peptide **5** with six lysines proved at least that electrostatic interactions were not the driving forces of the recognition process. Comparison of peptides **2**, **5** and **6** suggests a crucial role for the C-terminal tryptophan in either the three-dimensional structure of the peptide or in the binding to dsDNA. With peptide **6**, the fluorescence was decreased to about 30% of the initial value and did not change even after addition of 0.1 mM concentration. Using the peptide concentration that caused half of the total (70%) fluorescence decrease its affinity was calculated as $K_a = 2.8 \pm 1.1 \times 10^6$ M^{-1}, a value in the same order of magnitude, when compared to peptide **2**. The same behaviour was observed with peptide **7**, for which $K_a = 4.7 \pm 3.6 \times 10^6$ M^{-1} was calculated. Peptide **7** is a 16-residue peptide identical to peptide **2** except at the N-terminus, where the Cys(Npys) residue has been removed and the terminal arginine *N*-acetylated. The peculiar role played by the N-terminus Cys(Npys) residue (Fig. 1) in the binding process was clearly established by preparing and testing peptides **8** and **9**. In peptide **8**, the thiol function of the cysteine present in peptide **2** was protected with an *S*-acetamidomethyl group instead of the *S*-3-nitro-2-pyridinesulfenyl and the N-terminus amino function was acetylated, whereas in peptide **9** the original Npys group was maintained, but the N-terminus amino function was acetylated to avoid a possible N,S shift of Npys. Peptide **8** with an Ac-Cys(Acm) residue behaves as peptides **6** and **7**, with a plateau at 60 to 70% decrease of fluorescence, with $K_a = 5.5 \pm 4.9 \times 10^6$ M^{-1}, whereas peptide **9** with an Ac-Cys(Npys) residue has exactly the same behaviour as peptide **2**, that is the fluorescence of the dsDNA–BET complex was totally abolished, and no plateau around mid-point displacement was detected. Peptide **9** has an affinity $K_a = 5.5 \pm 2.1 \times 10^6$ M^{-1}, a non significant decrease compared to peptide **2**. The identical K_a values for peptides **8** and **9** may suggest that the *S*-3-nitro-2-pyridinesulfenyl does not give a significant contribution to the binding strength of these major groove binding peptides, but instead, enhances the binding site size, since it displaces the residual ethidium bromide still intercalated in the dsDNA. As a general comment, we must add that all the calculated affinity values, lower ones in particular, may be overestimated (see below the results obtained with the gel shift assay), since we used for their calculation the competitive binding model.[1]

The role of the nitropyridinesulfenyl protecting group (Fig. 1) was further ascertained. Firstly, we demonstrated that the amino acid Cys(Npys) itself was able to reduce the fluorescence of the prebound ethidium bromide from 100% to 40–30%, with an apparent $K_a = 0.3 \pm 0.1 \times 10^6$ M^{-1}. We had previously synthesized a N-terminus Cys(3-nitro-2-pyridinesulfenyl)-substituted SP analogue, peptide **10**, in the course of our structure–affinity relationship with the Substance P receptor. Substance P is an amphiphilic peptide with three positive net charges at the N-terminus, which has no ability to displace ethidium bromide from the preformed dsDNA–BET complex, even with concentrations up to 0.1 mM, (Table 1). Interestingly [Cys(Npys)^0]Substance P, peptide **10**, binds to dsDNA (G1/C2) and totally displaces the ethidium bromide with a $K_a = 1.2 \pm 0.4 \times 10^6$ M^{-1}. Thus, the 3-nitro-2-pyridinesulfenyl group and Substance P act in synergy being both necessary to completely displace the ethidium bromide bound to dsDNA. [Cys(Npys)^0]-Substance P is only about 5-times less potent than peptide **9**. A possible explanation for the role of the 3-nitro-2-pyridinesulfenyl group could be that this charged aromatic moiety intercalates within the base-pairs and forces Substance P to bind to DNA either in the minor or in the major groove.

However, the major aim of this study was not to demonstrate the exact role of the 3-nitro-2-pyridinesulfenyl group but to establish that the FID assay, which is an efficient and rapid method to screen minor groove binding molecules, could also be applied to major groove binding peptides. Thus, we compared the K_a values obtained for peptides **8** and **9** with this FID assay and the affinities (EC_{50} values) of these peptides for the 12-base-pair dsDNA G1/C2 measured by gel mobility shift assay.

Gel retardation assay

The binding affinities of peptides **8** and **9** were analyzed by PAGE using the radiolabelled G1/C2 duplex or a longer DNA target, 178-bp, containing more than one potential binding site for the *Antp* helix 3 homeodomain (Table 2). When the 12-base-pair dsDNA (G1/C2) was combined with increasing amounts of peptides **8** or **9** no retarded species were detectable in the gel,

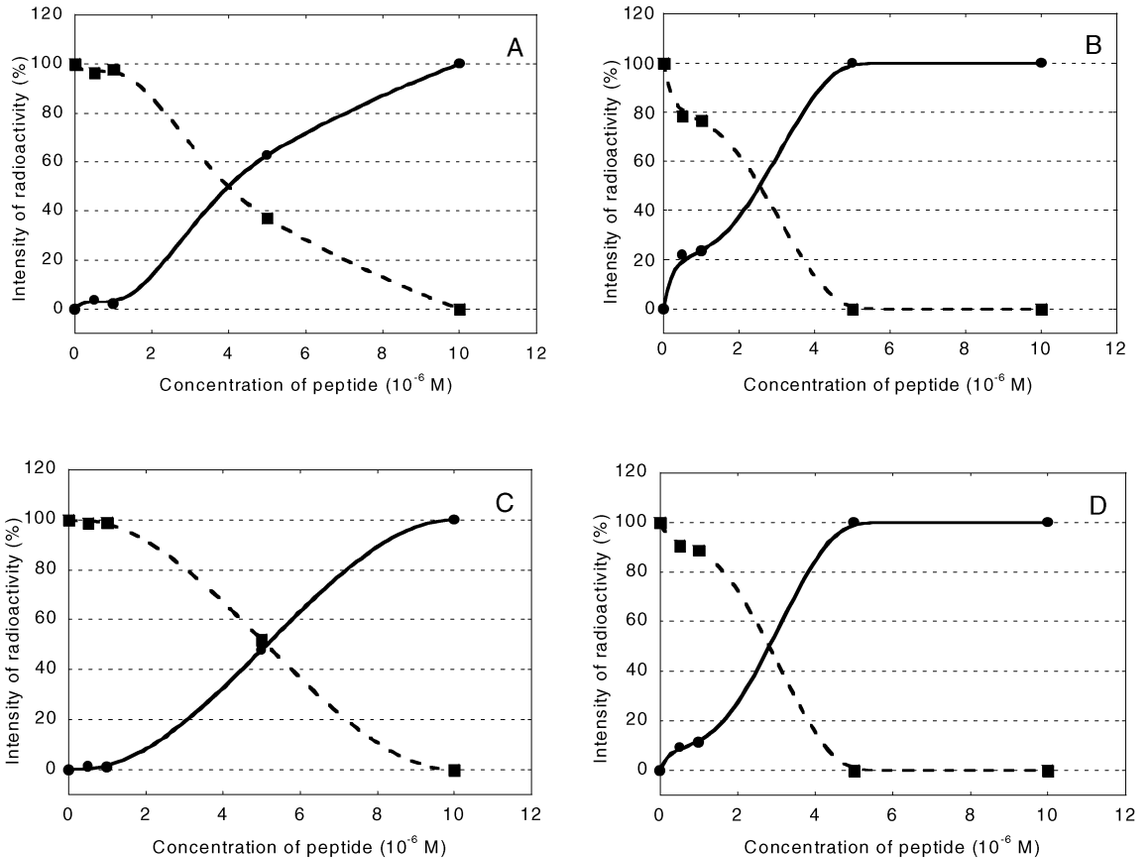

Fig. 3 Typical titration curve of a 12-bp dsDNA fragment (G1/C2, Table 2) with peptides **8** or **9**. The radiolabelled duplex (10×10^{-9} M) was incubated for 3.5 h in binding buffer (20 mM Tris-HCl, pH 7.6, 75 mM KCl, 50 μg mL^{-1} BSA, 10% glycerol), containing increasing concentrations of peptide **8** or **9** at 4 °C. Electrophoresis was performed on a 15% polyacrylamide gel (19 : 1 acrylamide–bisacrylamide) in 0.5 × TBE buffer solution at 300 V, 4 °C, which was preheated for 2 h at 300 V, 4 °C. The amounts of radioactivity remaining in the wells (●, ——) and of the duplex in the gel (■, - - -) are reported as a function of peptide concentrations. A) and B) with peptides **8** and **9**, respectively; the amount of radioactivity corresponding to the dissociated sDNA was not included in the calculations: the radioactive dsDNA and the radioactivity in the wells corresponds to 100%. C) and D) with peptides **8** and **9**, respectively; the amount of radioactivity corresponding to the dissociated sDNA was included in the calculations.

but we constantly found a decrease in the radioactivity associated with the free, running, duplex and a concomitant increase of radioactivity in the wells. Interestingly, Herdewijn *et al.*[19] reported that with some "unnatural" oligopeptides a distinguished retarded band for the DNA–oligopeptide complex was not observed, but just a smear, and they estimated the binding affinities for their peptides by measuring the residual amount of free radiolabelled DNA. In contrast to their report, we did not observe a smear, but the total radioactivity in each lane could be accounted for by adding that of the free dsDNA to that of the material remaining in the well. Despite much effort, we were unable to find conditions that induce migration in the gel of the material remaining in the wells, whose associated radioactivity was found to correlate with the peptide concentrations. In Fig. 3, it is reported, for each lane in the gel, the percentage of the radioactivity of the dsDNA band and that present in the corresponding well as a function of peptide concentrations. The intercepts of these curves around 50% for both peptides **8** and **9** gave the EC_{50} values: $EC_{50} = 4.0 \pm 1.1 \times 10^{-6}$ M was found for peptide **8**, which in the FID assay displaces only about 70% of the bound ethidium bromide and a slightly higher affinity, $EC_{50} = 2.5 \pm 0.3 \times 10^{-6}$ M, for peptide **9**, which, in the FID assay, totally displaces ethidium bromide. Since this short 12-base-pair dsDNA spontaneously dissociated in part during electrophoresis, we repeated the experiments with a 178-bp duplex containing different hypothetical binding sites for *Antp* HD, (Table 2, underlined sequences). Again, it was found that increasing amounts of the radiolabelled target duplex remained in the wells in the presence of increasing concentrations of peptides **8** or **9**. The estimated EC_{50} mean values from several experiments are $EC_{50} = 1.7 \pm 1.1 \times 10^{-6}$ M for peptide **8** and, as with G1/C2 dsDNA, a slightly higher affinity for peptide **9**, $EC_{50} = 0.7 \pm 0.1 \times 10^{-6}$ M. A typical electrophoretic mobility shift experiment and a titration curve are shown in Fig. 4 and Fig. 5, respectively.

Table 3 EC_{50} values from PAGE experiments

Duplex target	Peptide **8** $EC_{50}/10^{-6}$ M [a]	Peptide **9**
G1/C2	4.0 ± 1.1	2.5 ± 0.3
178	1.7 ± 1.1	0.7 ± 0.1

[a] EC_{50} values were calculated as described in Experimental section.

Altogether these data confirm the results obtained with the FID assay, showing that peptides **8** and **9** have similar affinity values, in the 0.1 to 1 micromolar range. Peptide **9** binds about 3-times more strongly the 178-bp DNA fragment (Table 3), containing more than one potential binding site. Different incubation times did not change the EC_{50} values, no difference was observed between 15 min, 2 h and 24 h for the 178-bp target, and between 3.5 and 24 h for the G1/C2 duplex, indicating that equilibrium was rapidly reached (data not shown). These K_a or EC_{50} values can be regarded just as relative values that allow a comparison only within the same family of peptides (Table 3).

Some of the peptides listed in Table 1, peptides **4**, **5**, **10** and Substance P, have also been rapidly screened, (only three concentrations 0.1, 1 and 10×10^{-6} M), in this gel retardation assay with the G1/C2 duplex. Data obtained are also in agreement

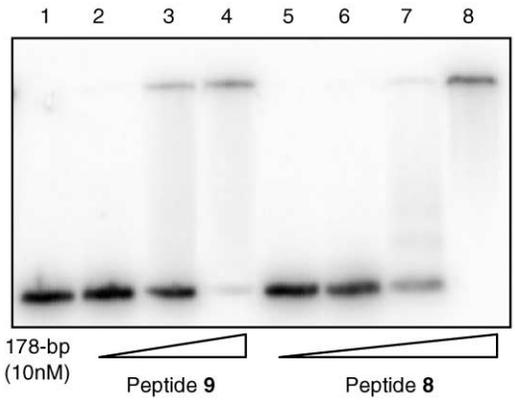

Fig. 4 Electrophoretic mobility shift assay of a 178-bp DNA fragment (Table 2) in the presence of peptide **8** or **9**. The 178-bp duplex target (lane 1) was incubated with increasing concentrations of peptide **9** (0.1×10^{-6} M, 0.5×10^{-6} M and 1×10^{-6} M, lanes 2–4) and **8** (0.1×10^{-6} M, 0.5×10^{-6} M, 1 and 5×10^{-6} M, lanes 5–8). The samples were incubated for 1 h at 4 °C in 20 mM Tris-HCl, pH 7.6, 75 mM KCl, 50 μg m^{-1}L BSA, 10% glycerol and loaded on a 1.5% agarose gel in 0.5 × TBE buffer, and run at 25 °C for 30 min at 180 V.

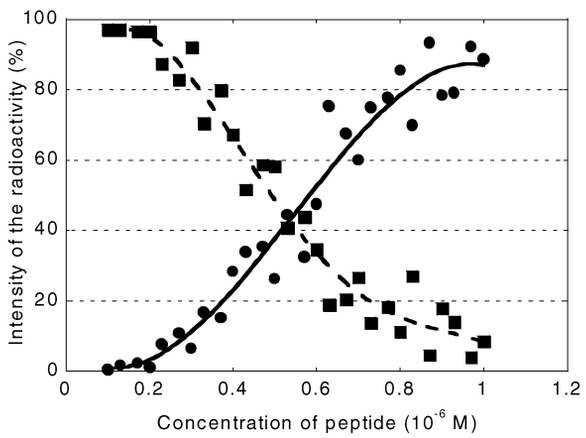

Fig. 5 Titration curve of a 178-bp DNA fragment (Table 2) with peptide **9**. The 178-bp at a 10×10^{-9} M concentration was incubated for 2 h in binding buffer (20 mM Tris-HCl, pH 7.6, 75 mM KCl, 50 μg mL^{-1} BSA, 10% glycerol), containing increasing concentrations of peptide **9** at 4 °C. Electrophoresis was performed on a 6% polyacrylamide gel (19 : 1 acrylamide–bisacrylamide) in 0.5 × TBE buffer solution at 300 V, 4 °C, which was preheated for 1 h at 300 V, 4 °C. The amount of radioactivity in the wells (●, ——) and of the unbound duplex (■, ---) is reported as a function of peptide concentrations. In this experiment we can estimate that the intercept of these curves yields an EC_{50} of peptide **9** of 0.54×10^{-6} M.

with the affinities reported in Table 1. Peptide **4** even at 10×10^{-6} M, the highest concentration used for peptide **8** and **9**, did not decrease the amount of radioactivity corresponding to the free dsDNA band. Peptide **5** and Substance P, at 1 and 10×10^{-6} M, respectively, bound the G1/C2 duplex, part of the labelled dsDNA remaining in the well. Peptide **10**, [Cys-(Npys)^0]SP, was more potent than Substance P, at the lowest concentration used (0.1×10^{-6} M) radioactivity was already found in the well and at 10×10^{-6} M free dsDNA was no longer detectable.

Footprinting assay

In order to investigate the binding specificity, we performed DNase I-footprinting experiments on the 178-bp DNA fragment. The target, incubated in the absence or in the presence of increasing concentrations of peptides **8** or **9**, was digested partially by DNase I and separated by gel electrophoresis in denaturing conditions. The differential cleavage plots, shown in Fig. 6, clearly reveal the binding sites of these peptides. Peptides **8** and **9** show enhanced cleavage inhibition at TTTCCC (site 1), TAATAC (site 4), CTATAG (site 5), AATTGG (site 6) sites. The footprints coincide with the position of AT-rich sequences, and, as expected, the sequence TAATAC (site 4) was one of the most protected site, the strongest being site 5 (CTATAG). The other potential binding site (Table 2) is in a region that cannot be analysed. The inhibition of DNase I DNA cleavage increases as the concentration of peptide increases. Peptide **9** has a better affinity for the 178-bp DNA fragment than peptide **8**: 10 μM of peptide **8** are needed to obtain a strong footprint while only 1 μM is needed for peptide **9**. It is worthy of note that peptide **8** binds only weakly to sites 2 and 3 bearing the least favorable DNA binding sequences (ACGTTG, GAGCGC, respectively) and appears more specific than the Cys(Npys)-substituted peptide **9**. These results are in perfect agreement with the behaviours of peptides **8** and **9** in the FID assay. Clearly, Cys(Npys) must interact within the duplex, and some of the protection observed (sites 2 and 3) with peptide **9** and not observed with peptide **8** must be induced by the presence of this thiol protecting group.

Conclusion

The present work demonstrates that the fluorescence intercalator displacement (FID) assay described by Boger *et al.*[1] to measure binding affinities of minor groove DNA binders is also suitable to evaluate rapidly the potencies of peptides binding in the major DNA groove. In analogy with the behaviour of some minor groove binders described very recently by Boger *et al.* [20] some of the investigated *Antp* helix 3 analogues displace only a fraction of the bound ethidium bromide, with a final fluorescence value around 40 to 30% of the initial value. This 100 to 40–30% decrease appears, however, sufficient enough to calculate apparent affinities or relative affinities, if this FID assay is to be set up as a high-throughput screening assay, for minor and major groove binders alike. The micromolar affinities (from 10^{-6} to 10^{-7} M) of *Antp* helix 3 analogues were confirmed by gel mobility shift and they are in the range reported by Montclare and Schepartz[21] for the helix 3 of Engrailed protein. Preliminary indications of the binding selectivity were obtained by DNase I footprinting assay, showing a clear preference for AT rich sites. During the course of this study we found that the 3-nitro-2-pyridinesulfenyl moiety binds to DNA with a micromolar affinity and is even capable of directing within DNA grooves a peptide with no affinity for DNA. This serendipitous discovery has now to be further explored.

Experimental

General chemicals

All the chemicals and solvents used for peptide syntheses were from Acros Organics (France) and Senn Chemicals AG (Switzerland) and peptide syntheses were performed on an ABI 433A peptide synthesizer (Applied Biosystems). Acetonitrile for HPLC was analytical gradient grade purchased from VWR. Water used for HPLC purifications was obtained from a Milli-Q system (Millipore). Ethidium bromide and distamycin A were obtained from Aldrich. All reagents were used without further purification.

Oligonucleotides

Oligonucleotides G1 and C2 were purchased from Proligo France SAS (Guaranteed™ oligos) as solutions in water and were stored as stock solutions at −80 °C. Concentrations were determined spectrophotometrically at 25 °C using molar extinction coefficients at 260 nm calculated from a nearest-neighbor model.[22] The radiolabelled G1/C2 target duplex was obtained by labelling at the 5′- end, one strand at a time, with [γ-^{32}P]ATP

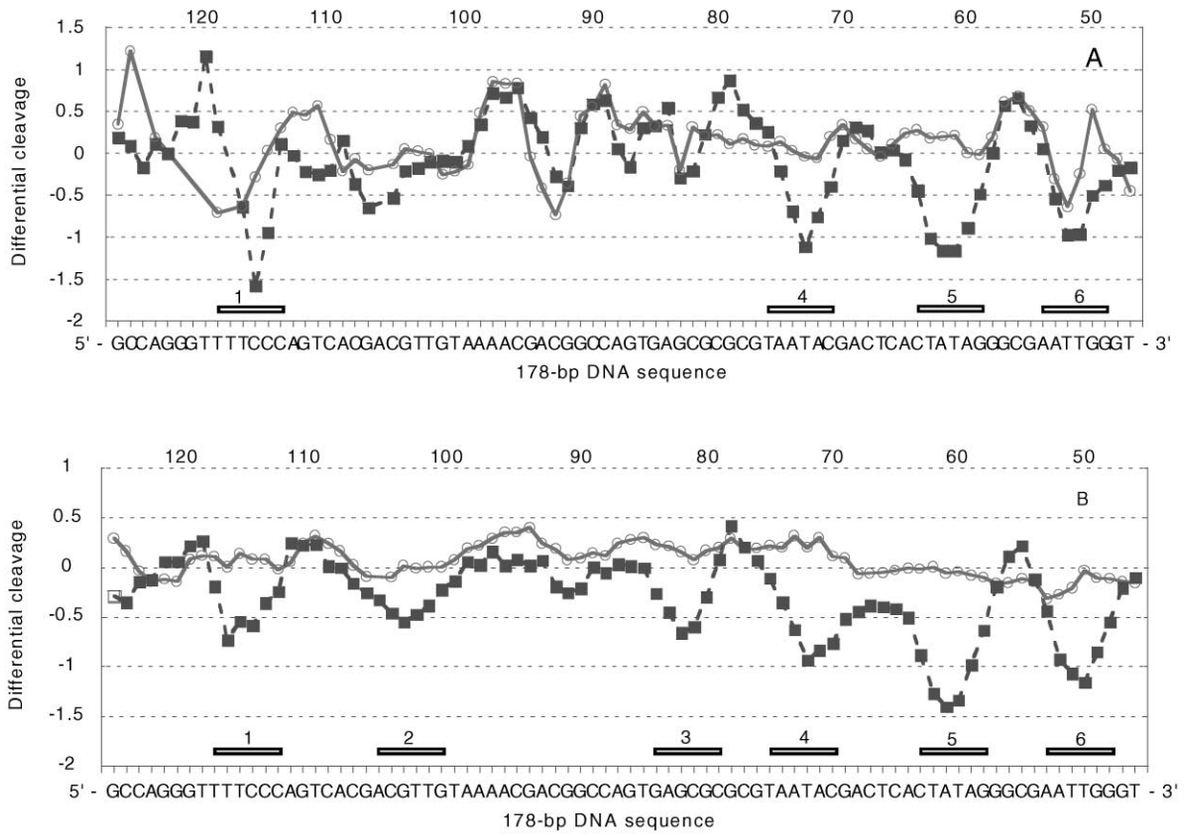

Fig. 6 Differential cleavage plots comparing susceptibility of the 3′-end radiolabelled 178-bp DNA fragment (Table 2) to DNase-I cutting in the presence of (A) 1×10^{-6} M (○) and 10×10^{-6} M (■) concentrations of peptide **8** and (B) 0.1×10^{-6} M (○) and 1×10^{-6} M (■) concentrations of peptide **9**. Negative values correspond to a ligand-protected site, and positive values represent enhanced cleavage. Vertical scales are in units of ln(*fa*) − ln(*fc*), where *fa* is the fractional cleavage at any bond in the presence of the peptide and *fc* is the fractional cleavage of the same bond in the control given closely similar extents of overall digestion. Each line drawn represents a 3-bond running average of individual data points, calculated by averaging the value of ln(*fa*) − ln(*fc*) at any bond with those of its nearest neighbours. Only the region of the restriction fragment analysed by densitometry is shown. Boxes indicate the positions of inhibition of DNase I cutting in the presence of the peptide.

(Amersham, France) using T4 polynucleotides kinase (New England Biolabs, France), followed by incubation with the complementary non-labelled strand for 5 min at 90 °C and hybridisation upon slow cooling to room temperature. The radiolabelled 178-bp DNA fragment was obtained by digestion of plasmid pBSK(±) (Promega, USA) by *Pvu*II and *Eco*R I, yielding a fragment suitable for 3′-end labelling by the Klenow polymerase and α-[^{32}P] dATP (Amersham, USA). The detailed procedures for isolation, purification and labelling of this duplex DNA fragment have been previously described.[23]

Peptide synthesis

Peptide synthesis was carried out on a 0.1 mmol scale on an ABI Model 433A Peptide Synthesizer (Applied Biosystems), starting with *p*-methylbenzhydrylamine resin (MBHA resin, typical substitution 0.9 mmol g^{-1} of resin). Standard protocols for *tert*-butyloxycarbonyl (Boc) protected amino acids were used. After removal of the last N-α-Boc protecting group, the resin was dried *in vacuo*. Peptidyl-MBHA-resin was treated with liquid HF at −20 °C (30 min) and 0 °C (30 min) in the presence of 1.5 mL of anisole and 0.25 mL of dimethyl sulfide per gram of peptidyl-resin. After evaporation *in vacuo* of HF and the solvents, the resin was washed three times with ether and then subsequently extracted three times with 10% AcOH. Lyophilisation of the extract gave the crude peptides which were purified by preparative reverse phase high performance liquid chromatography (HPLC) with an Applied Biosystems HPLC using a Perkin Elmer Prep-10 octyl 20 μm 10.0 × 250 mm column or Waters SymmetryPrep™ C_8 7 μm, 7.8 × 300 mm column. The purification was accomplished with acetonitrile gradients in aqueous trifluoroacetic acid (0.1%) at a flow rate of 6 mL min^{-1} with UV detection fixed at 220 nm. Analytical control of individual fractions was carried out using reversed phase analytical HPLC on Waters Symmetry® C_8 5 μm, 4.6 × 250 mm column in isocratic or gradient mode with acetonitrile and aqueous trifluoroacetic acid (0.1%) at a flow rate of 1.5 mL min^{-1} with a Waters 600 pump system and a Waters 2487 detector fixed at 210 nm. The identity of the peptide was confirmed by Matrix Assisted Laser Desorption Ionisation Time-Of-Flight (MALDI-Tof) mass spectroscopy in the positive ion mode using α-cyano-4-hydroxycinnamic acid as matrix. Peptide **2**: yield 33%; purity 94.2%; MALDI-Tof: MH^+ found 2348.23 (calcd. 2504.1, the Npys group is cleaved with the MALDI-Tof conditions, as already observed with all the Cys(Npys)-substituted peptides prepared in the laboratory); analytical HPLC: isocratic mode, 21% CH_3CN in 0.1% TFA, t_R = 15.94 min. Peptide **3**: yield 14%; purity 96.4%; MALDI-Tof: MH^+ found 1447.83 (calcd. 1447.79); analytical HPLC: isocratic mode, 16% CH_3CN in 0.1% TFA, t_R = 13.97 min. Peptide **4**: yield 16%; purity 99.4%; MALDI-Tof: MH^+ found 1873.97 (calcd. 1874.26); analytical HPLC: isocratic mode, 20% CH_3CN in 0.1% TFA, t_R = 7.17 min. Peptide **5**: yield 17%; purity 100%; MALDI-Tof: MH^+ found 2216.39 (calcd. 2216.27); analytical HPLC: isocratic mode, 30% CH_3CN in 0.1% TFA, t_R = 7.03 min. Peptide **6**: yield 26.4%; purity 98.8%; MALDI-Tof: MH^+ found 1890.15 (calcd. 1890.35); analytical HPLC: isocratic mode, 16% CH_3CN in 0.1% TFA, t_R = 13.15 min. Peptide **7**: yield 34.8%; purity 89.0%; MALDI-Tof: MH^+ found 2287.27 (calcd. 2287.23); analytical HPLC:linear gradient of CH_3CN from 24 to 48% in 30 min in 0.1% TFA, t_R = 16.0 min. Peptide **8**: yield 50.4%; purity 98.7%; MALDI-Tof: MH^+ found 2461.42 (calcd. 2461.38); analytical HPLC: isocratic mode, 16% CH_3CN in 0.1% TFA, t_R = 9.57 min. Peptide **9**: yield 28.4%; purity

99.2%; MALDI-Tof: MH^+ found 2390.27 (calcd. 2544.39, the Npys group is cleaved with the MALDI-Tof conditions, as already observed with all the Cys(Npys)-substituted peptides prepared in the laboratory); analytical HPLC: isocratic mode, 16% CH_3CN in 0.1% TFA, t_R = 16.55 min.

Ethidium bromide assay

Oligonucleotides 10 μL (final concentration 0.88×10^{-5} M base pairs) were mixed with ethidium bromide 88 μL (final concentration 0.44×10^{-5} M) in a 2 : 1 ratio base–ethidium bromide in a 0.1 M Tris-HCl, pH 8.0, 0.1 M NaCl buffer. After overnight incubation at 25 °C, aliquots of 7 μL were directly laid down on X63 Zeiss plan Neofluar objective (Zeiss, Oberkochen, Germany). Fluorescence measurements were made with the UV-visible spectofluorometer developed in the laboratory.[24] The excitation wavelength was the 514 nm line of an argon laser and the fluorescence emission was recorded at 595 nm. The beam power was reduced about 0.1 μW by the use of neutral density filters. All the measures within an experiment were performed in duplicate with two control samples for 100% fluorescence (no peptide) and 0% fluorescence (no DNA). The experiments were at least duplicated. Fluorescence readings are reported as % fluorescence relative to the controls.

Gel retardation assay

Increasing concentrations (0.1×10^{-6} M to 10×10^{-6} M) of peptide were added to 10 nM of radiolabelled duplex (either G1/C2 or 178-bp) in 20 mM Tris-HCl, pH 7.6, 75 mM KCl, 50 μg mL^{-1} BSA, 10% glycerol. The samples were incubated as indicated at fixed temperature (4–25 °C). Electrophoresis was performed on a non-denaturating 6% (for the 178-bp duplex) or 15% (for the G1/C2 duplex) polyacrylamide gel (19 : 1 acrylamide–bisacrylamide) or 1.5% agarose gel in 0.5 × TBE (0.05 M Tris-base, 45 mM boric acid, 0.5 mM EDTA). After electrophoresis, the gels were transferred to a Whatman 3MM paper, dried under *vacuum* at 80 °C and then analysed on the phosphorimager (Molecular Dynamics). The intercept of the curves corresponding to the percentage of the radioactive dsDNA band (free dsDNA) and that present in the corresponding well as a function of peptide concentrations yields a relative EC_{50} value for the peptide. Mean values of 2 to 4 experiments are reported.

DNase I footprinting

The radiolabelled 178-bp DNA fragment was incubated, for 15 min on ice, in a binding buffer (20 mM Tris-HCl, pH 7.6, 4 mM KCl, 2 mM $MgCl_2$, 0.5 mM EDTA, 1 mM $CaCl_2$, 50 μg mL^{-1} BSA) containing increasing concentrations of the desired peptide. Then, DNA was digested on ice for 3 min with 0.007 U (diluted in 20 mM Tris-HCl, pH 7.3, 20 mM NaCl, 1 mM $MgCl_2$, 2 mM $MnCl_2$) of DNase I (Sigma, Germany). The DNase I cleavage reaction was terminated by addition of 100 μL cold ethanol. After double precipitation in ethanol, the samples were suspended in 95% formamide and heated at 90 °C for 4 min, then cooled on ice for 4 min before loading onto a 30 min preheated denaturating 8% polyacrylamide gel (19 : 1 acrylamide–bisacrylamide) containing 7 M urea in 1 × TBE buffer solution. After 2 h electrophoresis at 65 W, the gel was transferred to a Whatman 3MM paper, dried *in vacuo* at 80 °C and then analysed on the phosphorimager (Molecular Dynamics). Adenine/guanine specific Maxam–Gilbert chemical cleavage reactions were used as markers.

Abbreviations

Acm: acetamidomethyl; *Antp* HD: *Antennapedia* homeodomain; bp: base pairs; BET: ethidium bromide; BSA: bovine serum albumin; Boc: *tert*-butyloxycarbonyl; dsDNA: double-stranded DNA; sDNA: single-stranded DNA; FID: fluorescent intercalator displacement; HPLC: high-pressure liquid chromatography; Npys: *S*-3-nitro-2-pyridinesulfenyl; Maldi-Tof: matrix assisted laser desorption-time of flight; MBHA: *p*-methylbenzhydrylamine; PNAs: peptide nucleic acids; TFA: trifluoroacetic acid; TBE: tris-base, boric acid, EDTA.

Acknowledgements

Dr Gérard Chassaing, Dr Fabienne Burlina and Dr Nicole Goasdoué are greatly acknowledged for fruitful discussions and technical advice.

References

1 D. L. Boger, B. E. Fink and M. P. Hedrick, *J. Am. Chem. Soc.*, 2000, **122**, 6382–6394.
2 J. M. Turner, S. E. Swalley, E. E. Baird and P. B. Dervan, *J. Am. Chem. Soc.*, 1998, **120**, 6219–6226.
3 N. T. Thuong and C. Hélène, *Angew. Chem., Int. Ed. Engl.*, 1993, **32**, 666–690.
4 P. E. Nielsen, M. Egholm, R. H. Berg and O. Buchardt, *Science*, 1991, **254**, 1497–1500.
5 W. J. Gehring, M. Affolter and T. Bürglin, *Annu. Rev. Biochem.*, 1994, **63**, 487–526.
6 A. Laughon, *Biochemistry*, 1991, **30**, 11357–11367.
7 E. Fraenkel and C. O. Pabo, *Nat. Struct. Biol.*, 1998, **5**, 692–697.
8 L. Pellizzari, G. Tell, D. Fabbro, C. Pucillo and G. Damante, *FEBS Lett.*, 1997, **407**, 320–324.
9 M. Affolter, A. Percival-Smith, M. Müller, W. Leupin and W. J. Gehring, *Proc. Natl. Acad. Sci. USA*, 1990, **87**, 4093–4097.
10 D. Derossi, G. Chassaing and A. Prochiantz, *Trends Cell Biol.*, 1998, **8**, 84–87.
11 D. Derossi, A. H. Joliot, G. Chassaing and A. Prochiantz, *J. Biol. Chem.*, 1994, **269**(14), 10444–10450.
12 K. T. O'Neil, J. D. Shuman, C. Ampe and W. F. DeGrado, *Biochemistry*, 1991, **30**, 9030–9034.
13 K. T. O'Neil and W. F. DeGrado, *Science*, 1990, **250**, 646–651.
14 A. R. Lajmi, M. E. Lovrencic, T. R. Wallace, R. R. Thomlinson and J. A. Shin, *J. Am. Chem. Soc.*, 2000, **122**, 5638–5639.
15 P. Chaltin, F. Borgions, A. Van Aerschot and P. Herdewijn, *Bioorg. Med. Chem. Lett.*, 2003, **13**, 47–50.
16 B. C. Baguley and E-M. Falkenhaug, *Nucleic Acids Res.*, 1978, **5**, 161–171.
17 A. R. Morgan, J. S. Lee, D. E. Pulleyblank, N. L. Murray and D. H. Evans, *Nucleic Acids Res.*, 1979, **7**, 547–569.
18 M. Müller, M. Affolter, W. Leupin, G. Otting, K. Wüthrich and W. J. Gehring, *EMBO J.*, 1988, **7**, 4299–4304.
19 P. Chaltin, E. Lescrinier, T. Lescrinier, J. Rozenski, C. Hendrix, H. Rosemeyer, R. Busson, A. V. Aerschot and P. Herdewijn, *Helv. Chim. Acta*, 2002, **85**, 2258–2283.
20 C. R. Woods, T. Ishii, B. Wu, K. W. Bair and D. L. Boger, *J. Am. Chem. Soc.*, 2002, **124**, 2148–2152.
21 J. K. Montclare and A. Schepartz, *J. Am. Chem. Soc.*, 2003, **125**, 3416–3417.
22 C. R. Cantor, M. M. Warshaw and H. Shapiro, *Biopolymers*, 1970, **9**, 1059–1077.
23 C. Bailly, C. OhUigin, C. Rivalle, E. Bisagni, J. P. Hénichart and M. J. Waring, *Nucleic Acids Res.*, 1990, **18**, 6283–6291.
24 F. Sureau, L. Chinsky, M. Duquesne, A. Laigle, P. Y. Turpin, C. Amirand, J. P. Ballini and P. Vigny, *Eur. Biophys. J.*, 1990, **18**, 301–307.